

Drone-based Monitoring of Sunflower Crops

Asparuh Atanasov¹⁾, Radko Mihaylov¹⁾, Svilen Stoyanov²⁾, Desislava Mihaylova³⁾, Peter Benov⁴⁾

1) – Technical University of Varna, Department of Mechanics and Elements of Machines, 9010, 1 Studentska Street, Varna, Bulgaria

2) – Technical University of Varna, Department of Manufacturing Technologies and Machine Tools, 9010, 1 Studentska Street, Varna, Bulgaria

3) – Technical University of Varna, Department of Electronic Technique and Microelectronics, 9010, 1 Studentska Street, Varna, Bulgaria

4) – Technical University of Varna, Dobrudzha Technological College, 12 Dobrotica Street, 9302, Dobrich, Bulgaria

Corresponding author contact: asparuh.atanasov@tu-varna.bg

Abstract Remote monitoring and utilization of digital technologies is essential for the application of the precision farming approach, which contributes significantly to the improved quality of agricultural products. The paper compares the data for six vegetation indices when observing the sunflower vegetation in South Dobrudzha in 2021. Images with RGB and digital NIR camera were obtained via a remotely piloted quadcopter. The flight plan specifies speed 8 m/s, altitude 100 m and shooting overlapping images of 80%. Six vegetation indices: NDVI, EVI2, SAVI, CVI, MGVI and MPRI were calculated from the images obtained during the flight. The calculation of the indices takes into account the intensity of solar radiation and the parameters of the meteorological situation at the time of shooting. The findings obtained reveal a stable trend of change of the vegetation indices, thus, establishing accurate and reliable results as for the monitoring of agricultural areas with unmanned aerial vehicles.

Keywords: agricultural monitoring, infrared imaging, sunflower, vegetation indexes, drone

1 Introduction

Monitoring the soil and tracking the vegetation process is crucial for precision farming. Numerous indices have been developed for different applications under all observation conditions, (Bannari et al. 1995). The values of the vegetation indices of the crops may be limited by various physical effects that affect the accuracy of the measurement. For example from: atmospheric parameters, (Myneni & Asrar, 1994); topographic factors, (Burgess et al. 1995); soil optical properties (Baret et al.1993), spatial and spectral characteristics of sensors (Teillet et al.1997) and problems of saturation and linearity of sensor-reported data, (Huete, 1988). Accordingly, these factors increase or decrease the reflections of solar radiation in the red and near-infrared spectral regions and make it difficult to detect changes in vegetation. This can cause errors in the interpretation and analysis of the results obtained by remote sensing. Most of these problems can be corrected by calibration to the conditions at the time of field measurement before the calculation of vegetation indices.

The following widespread vegetation indices were used in the present study:

NDVI - Normalized Difference Vegetation Index. Characterizes the density of vegetation, growth, the presence of weeds or diseases, helps to predict yields. The index is generated by images of green vegetation that absorbs electromagnetic waves in the visible red range of the spectrum and reflects them in the near infrared. The red region of the spectrum (0.62 - 0.75 μm) reports the maximum absorption of solar radiation by chlorophyll, and the near infrared zone (0.75 - 1.3 μm) has the maximum reflection of energy from the cellular structure of the leaves, [Rouse et al. 1974].

SAVI - Soil Adjusted Vegetation Index. Its formula is given in Table 1 where L is the regulating factor, (Huete, 1988) and has a value of $L = 0.5$, is the optimal correction factor for reducing the "noise" of the soil in the whole range of vegetation images. The multiplication factor $(1 + L)$ in front of the index is only needed to maintain the dynamic range of the index. The value of L becomes smaller in value when the vegetation is denser. For more precise studies, three correction factors are preferred : $L = 1$ for analysis of very low density vegetation; $L = 0.5$ for intermediate vegetation density, and $L = 0.25$ for higher densities, $L = 0.5$ is used in the present study.

EVI2 - Enhanced Vegetation Index 2. It can be used for sensors without a blue band, to obtain an EVI-like vegetation index, (Zhangyan et al. 2008), supplementing NDVI.

CVI - Chlorophyll Vegetation Index. It is hypersensitive to the content of chlorophyll in deciduous plants. It is used from the beginning to the middle of the crop growth cycle for a wide range of soils and sowing conditions. The increased sensitivity of the index to the concentration of chlorophyll in the leaves is due to the effective normalization of various values of LAI, (Leaf Area Index), (Watson, D.J. 1947) obtained with the introduction of red and green colors, (Vincini et al. 2008).

The MPRI - Modified Photochemical Reflectance Index is used to assess the variability of vegetation and soil, as it provides the best visual distinction between these variables. The MPRI index is dependent on cloud shading, the shadows of which can be associated as more developed plants compared to neighboring areas. When areas affected by variations in sunlight reflection are identified, they should be eliminated from the agronomic analysis used to assess the condition of the vegetation, (Yang et al. 2008).

MGRVI - Modified Green Red Vegetation Index also gives good results, as it can effectively distinguish vegetation and soil with results close to the results obtained visually by MPRI, (Bendig, et al. 2015).

This study aims to show the trends in the change of these vegetation indices when observing a sunflower field and to provide information on plant development that is useful for the needs of precision agriculture using a small UAV.

2 Materials and methods

The indices used in the present study and the formulas for their preparation are listed in Table 1. They are selected by popularity, for example - NDVI, and the possibilities for their generation according to the spectral characteristics of the camera with which the image is taken. The comparison of the indices contributes to increasing the reliability of the observation results.

Table 1. Vegetation indices and formulas by which they are calculated.

Index	Name	Formula	Author
NDVI	Normalized difference vegetation index	$(R_n - R_r)/(R_n + R_r)$	Rouse et al. (1974)
SAVI	Soil adjusted Vegetation Index	$(1 + 0.5) (R_n - R_r)/(R_n + R_r + 0.5)$	Huete, (1988)
EVI2	Enhanced Vegetation Index 2	$2.5*((R_n - R_r)/(R_n + 2.4*R_r + 1))$	Zhangyan et al. (2008)
CVI	Chlorophyll Vegetation Index	$(R_r * R_n)/(R_g)^2$	Vincini et al. (2008)
MPRI	Modified Photochemical Reflectance Index	$(R_g - R_r)/(R_g + R_r)$	Yang et al. (2008)
MGRVI	Modified Green Red Vegetation Index	$(R_g^2 - R_r^2)/(R_g^2 + R_r^2)$	Bendig, et al. (2015)

2.1. Place of observations

The place of the shooting is with geographical coordinates: 43.548925N, 27.761216E, field sown with sunflower variety: SY Onestar CLP of Syngenta on 25.04.2021 in the land of Dobrich, Bulgaria.



Fig. 1. Field plan, (map.google.com)

The flights were conducted from 05.05.2021 to 10.09.2021 at an interval of 10 days. Flies were made in 15 days during the observed period.

Observations on the vegetation of maize variety Decalp DX4541 / 370FAL sown in the field with coordinates: 43° 30' 46.156"N, 27° 40' 54.469"E are also made in the publication of, (Mihaylov, R., 2019). Flight height 100 m, Images captured by drone were taken in the months of April, May, June, July 2019. The data described are for vegetation indices obtained from a camera that registers only RGB reflection. Similar observations and calculation of vegetation indices obtained and data from NIR reflections have been published in, (Mihaylov, R., et al. 2020), both for maize and sunflower in different parts of South Dobrudzha, and the experience gained from them is the basis of the present study.

2.2. UAV Platform and Sensors

The flights were conducted with a quadcopter DJI Mavic 2 Pro. Its communication system consists of a duplex transmitter at a frequency of 2.4 GHz and a WiFi module at a frequency of 2.4 GHz for controlling the navigation of the unmanned aerial vehicle (UAV) and monitoring the flight parameters. The WiFi module provides video data transmission on a 5.8 GHz channel, providing a real-time image to control the terrestrial operator. The flight planning is realized by the software Pix4DCapture, (Pix4DCapture) which allows setting the route on parallel lines depending on the parameters of the video sensor and the set overlap of the photos in the direction of flight and in the transverse direction.

In addition to the UAV, a second MAPIR Survey3W Camera, (Mapir Camera Control), has been installed to capture images from the near-infrared area of solar radiation. The multispectral camera detects NIR reflections with a wavelength in the "near infrared" 850 nm, red - 660 nm and green - 550 nm spectrum of solar radiation.

Figure 2 shows a photograph of the observed field taken from a height of 100 m. The different angle of the photos is due to the differences in the angle of the cameras, as well as their optical characteristics.

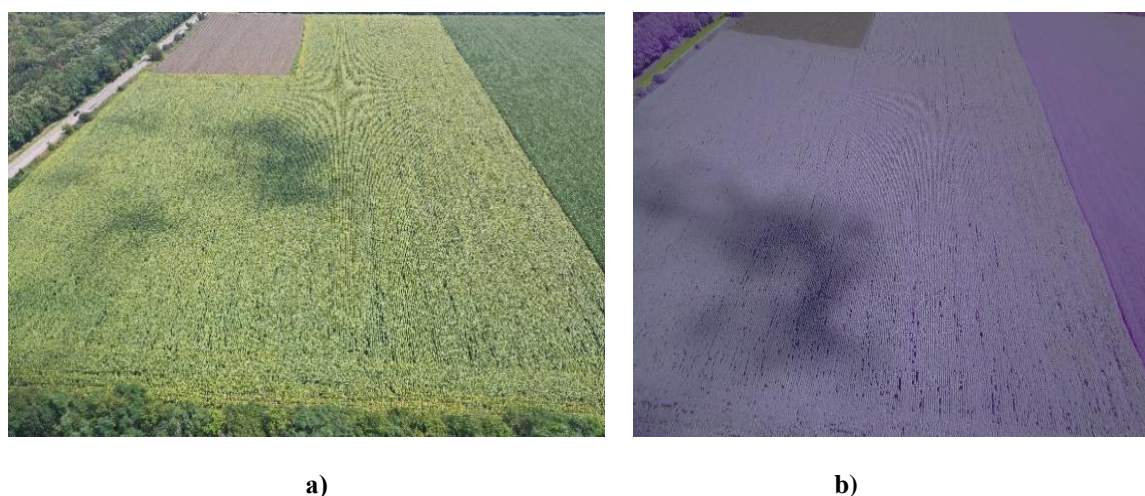


Fig. 2. Photos of the studied field with sunflower from 100 m height: a) with RGB camera and b) with NIR camera on 20.07.2021

A multispectral study at a height of 100 m above the ground with an overlap of 80% in both directions resulted in a resolution of 3.75 cm per pixel; size of the flight area 524 x 483 m; flight time 17.33 minutes. Travelled route along the route in the form of a meander 6518 m.

2.3. Multispectral Data Processing analyse

The image is calibrated and corrected, taking into account the lighting and the influence of the sensor a MAPIR calibrator, (Mapir Calibrating Application), is used. The corrections are applied to the camera parameters and the received information about the intensity of the solar radiation. By calibrating the sensor, the brightness is adjusted to obtain more accurate reflection values.

The data on the atmospheric conditions during the shooting are given in Table 2.

Table 2. Atmospheric conditions when shooting the field

Meteorological parameters	Dates in 2021												
	15.05.	25.05.	04.06.	14.06.	25.06.	30.06.	10.07.	20.07.	31.07.	11.08.	20.08.	30.08.	10.09.
Air temperature [°C]	22	20	20	16	30	25	28	28	31	26	25	22	20
Wind speed [m/s]	6,2	4,6	4,9	3,6	3,2	5	4,1	3,10	6,70	3,50	6,2	7,20	6,20
Wind direction	East	South east	Nord	West	Nord	South	Nord east	South	East	Nord	Nord	West	Nord
Humidity [%]	50	60	50	88	62	74	42	70	33	51	36	65	56
Sunlight [w/m ²]	454,8	188	98,9	130,9	-	333,1	167,1	162,2	353,4	144,1	148,2	184,2	238,8

2.4. Generation of Orthomosaic and the corresponding sparse Digital Surface Model, (DSM)

During the flight, the camera captures between 400 and 500 photos with a resolution of 4000x3000 pixels and saves them to SD card memory. Each photo is taken with a focal length of 3.0 mm, a speed at which the camera aperture opens and closes to let in a certain amount of light 1/500, a focal length of $f / 2.8$ and ISO 100. The planned pixel resolution is 2.34 cm according to the flight plan, and after processing with the Pix4D application program, [Pix4Dmapper] of overlapping images was obtained 3.75 cm per pixel. These images provide the raw data needed to create a series of maps / models and visualizations using Pix4Dmapper software. The image quality check after the initial processing gives an average value of 35,983 key image points. The relative difference between the original camera with the image parameters and its optimized parameters is 0.053%, which is well below the recommended variation, i.e., deviation of the parameters from the ideal value, of 5%. Programme calculated 14,206 matches of the calibrated image and determined an average RMS error of 0.092 m for the ground control points. The total number of image overlaps is in the range of 5+ for almost the entire target area above the field.

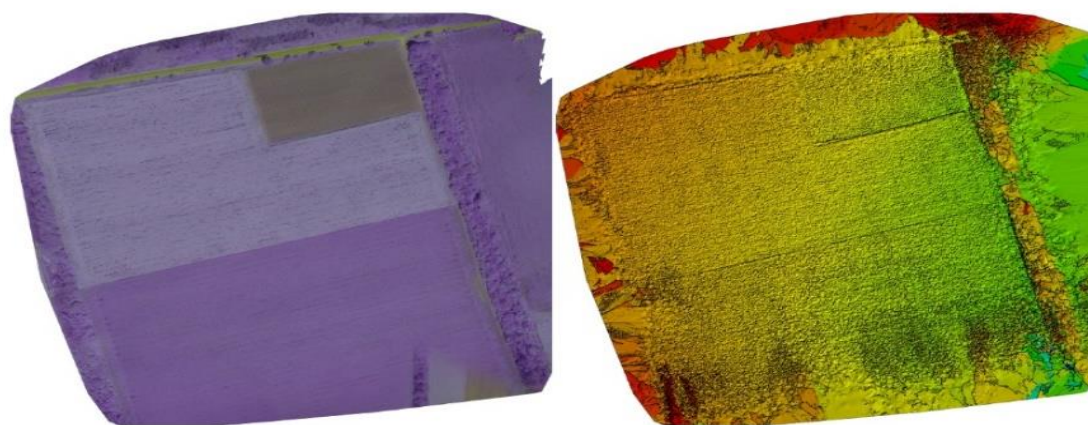


Fig. 3. Orthomosaic and the corresponding sparse Digital Surface Model (DSM) before densification, [Pix4Dmapper] from 20.07.2021 г.

3 Results

Results on the use of UAV to collect phenotypic data for multiple cultures have been published in the literature, (Sankaran et al., 2015; Shi et al., 2016; Yang et al., 2017, Mihajlow & Ivanova, 2019). Considered in the present paper is the use of a UAV-based multispectral monitoring system to identify sunflower vegetation. Field experiments show a close relationship between the observed variables and

the subsequent development of sunflower. This is a key aspect of new variety programs that aim to select plants of better quality and higher grain yields.

The field surveys made in the observation period are in 15 days, 13 of them generated the orthomosaic of the respective (DSM) before compaction. Vegetation indices are calculated from the raw data thus obtained.

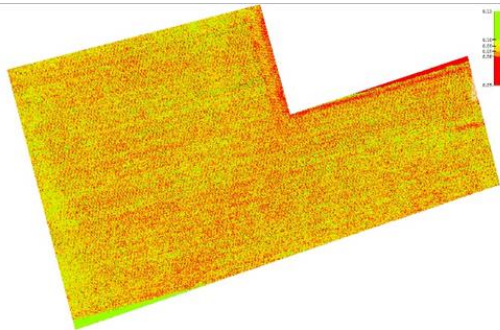


Fig. 4. NDVI reflection map from 20.07.2021

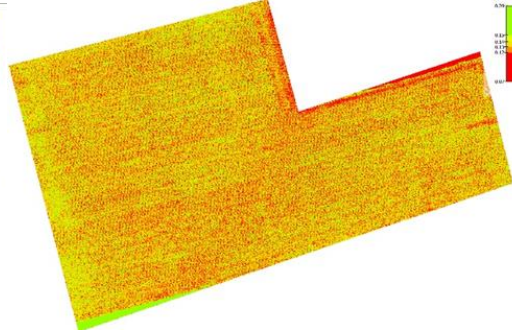


Fig. 5. EVI2 reflection map from 20.07.2021

Figures 4 and 5 show the generated reflection maps for calculating the NDVI and EVI2 indices. The similarity of the two cards is clear. The zones with the lowest value of the vegetation indices are in red, and in the lower corner with the highest in green. The difference between the two indices is only in the absolute values, but the tendency of change and the zones of low and high value of the vegetation indices overlap.

The results of the obtained reflectance indices for the whole vegetation period based on multispectral images are presented in Figures 6 to 9 with their respective minimum and maximum values.

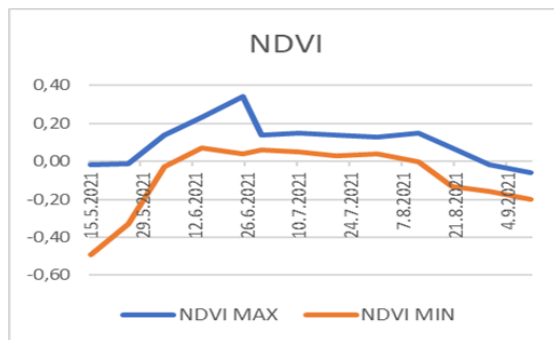


Fig. 6. Change of NDVI by date.

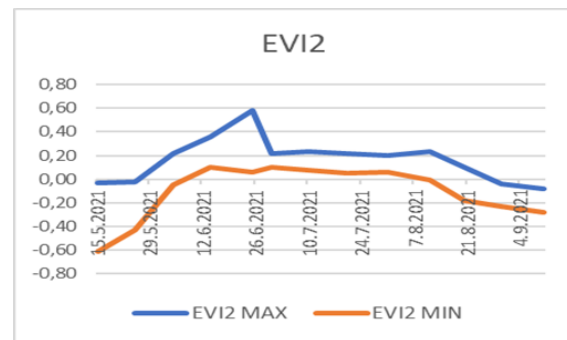


Fig. 7. Change of EVI2 by date.

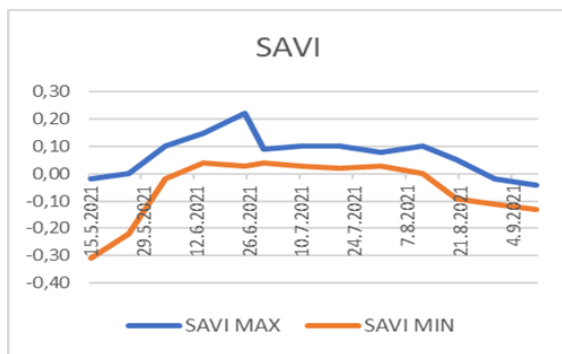


Fig. 8. Change of SAVI by date.

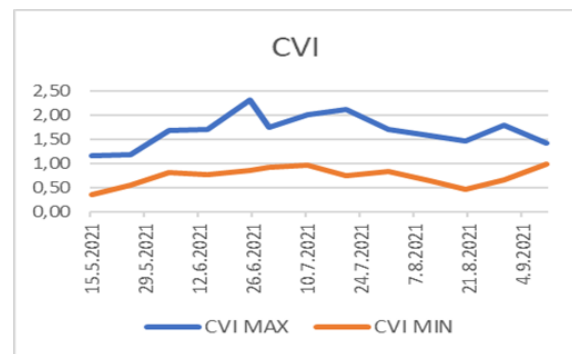


Fig. 9. Change of CVI by date.

The EVI2 index is complementary to the NDVI, leading to similar results in the trend. The CVI index due to its higher sensitivity to chlorophyll, (Vincini et al. 2008) is adapted for observation in the initial

stage of growth. For this reason, there are slight deviations from other indices in the period of sunflower ripening. In this case, it confirms the accuracy of the data for NDVI, EVI2. The SAVI index is optimized to eliminate soil noise, (Huete, 1988). Because the sunflower tightly covers the field, the value of the correction term in the equation L becomes 1, which gives similar values and trends with NDVI. On the whole, all indices listed hereto show the same trend and each of them is applicable to this type of observation.



Fig. 10. Change of MPRI by date.

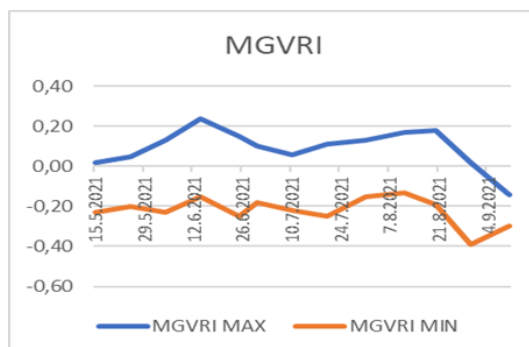


Fig. 11. Change of MGVRI by date.

Similar trends are shown by the indices based on RGB, (Fig. 10 and Fig. 11) the change in the line of the graph follows a similar pattern of change, although their numerical values differ. As a result, MGRVI showed higher contrast due to more negative and shaded pixels due to noise and shadows. It is more sensitive to shadows and noise than the leaves, i.e. not suitable for use in shaded areas and in variable clouds. Shows higher sensitivity than MPRI.

The comparison of the considered indices was made to confirm the accuracy of the results. Although there are some differences between the input data on which the observation was made, such as sunlight, humidity and other external environmental factors that lead to changes in the values of the images obtained. It is important to enter image data to calibrate and update the model. This, in turn, proves conclusively that the method employed for the purposes of the present study is highly suitable for the real environment, and validates its resistance to the influence of various external factors.

Figure 12 shows the minimum and maximum value of the NDVI index against the background of changes in meteorological parameters. The trends in the change of the vegetation index are directly related to them. During drought, the index decreases and is directly affected by the amount of precipitation and air temperature. This clearly indicates that the reported decrease in the reflection of near-infrared light is registered due to water and temperature stress in sunflower plants. On that account, the result achieved, confirms the applicability of the monitoring methodology. The tendency of change in the vegetation of the observed crop is visible, related to the influence of water reserves in the soil and air temperature.

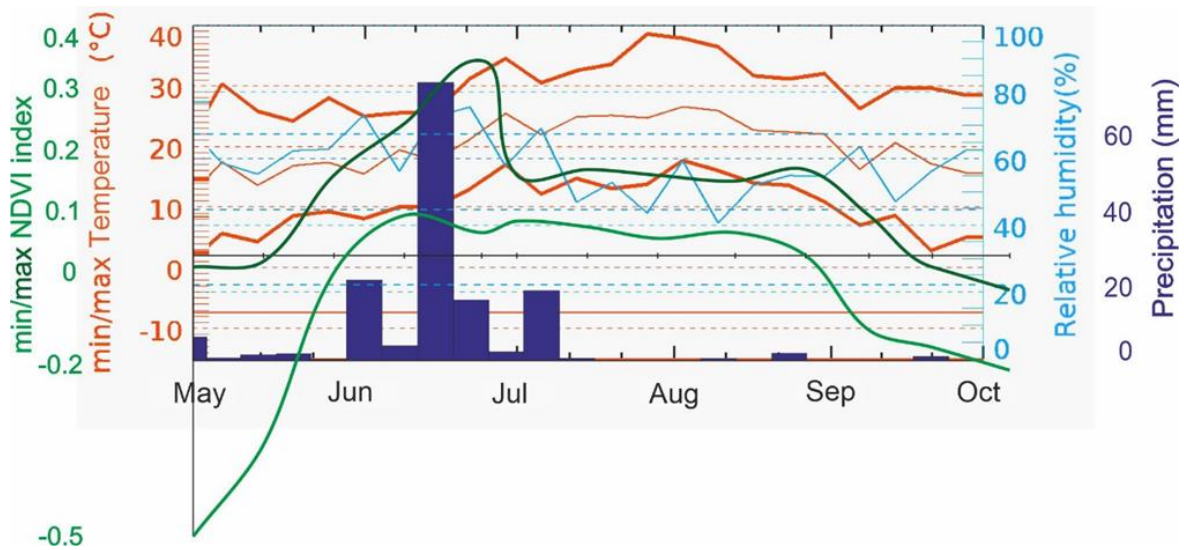


Fig. 12. Change in NDVI in a sunflower field against the background of changes in meteorological parameters.

4 Conclusions

More than 15,000 photos were taken during the 31 flights. In the course of observation, they were processed to obtain vegetation indices. The results present the segmentation coefficients, [Pix4Dmapper] for NIR multispectral data reach 0.92033 and 0.9531, respectively. The model is applied to the overall image obtained from the UAV and the output is the threshold for obtaining a segmented image.

The yield obtained from the observed field is 2700 kg/ha, which corresponds to the reported positive trends of change of the vegetation index NDVI until September 2021, (Fig. 12).

With images and a small UAV, the farmer can track and analyse crop data without being dependent on satellite images. Flying at an altitude of up to 100 m UAV is under the cloud cover, which makes it applicable in dense clouds in contrast to satellite observation. Meteorological features in the region of South Dobrudhza do not affect the collection of information with UAV.

Provided, additionally, in the paper is a contrast between the tendencies of change of six vegetation indices and their applicability in estimating the plant mass and crop yield forecasting.

The reliability of the results of remote sensing shows a direct dependence on precipitation, air temperature and vegetation of the observed sunflower. It is, further, possible to trace the effect of meteorological features on the influence of reflective vegetation indices, obtained with UAV multispectral images, (Fig. 12).

This study achieves optimal results by using a high-resolution digital camera to obtain images from the experimental sunflower field using UAV. It proved the applicability of the methodology for obtaining vegetation indices from sunflower areas with a size of 0,2 to 0,5 hectares.

The phenological data examined in the paper was acquired by recording reflections from specific spectral regions (i.e. the possibility of calculating vegetation indices) and hold reliable preliminary information for predicting the biomass content and potential of the studied plants, which will be the subject of subsequent research analyses.

Acknowledgments

The current study is funded by the budgetary subsidies of the Technical University of Varna for research and development activities related to the scientific project “HII9/2021”.

References

- Baret, F., Jacquemoud, S. & Hanocq, J. F. (1993). The Soil Line Concept in Remote Sensing. *Remote Sensing Reviews*, 7(1), 65-82. <https://doi.org/10.1080/02757259309532166>

- Bannari, A., Morin, D., Huete, A.R. & Bonn, F. (1995). Are view of vegetation indices. *Remote Sensing Reviews*, 13(1-2), 95-120. <https://doi.org/10.1080/02757259509532298>
- Bendig, J., Yu, K., Aasen, H., Bolten, A., Bennertz, S., Broscheit, J. & Bareth, G. (2015). Combining UAV-based plant height from crop surface models, visible, and near infrared vegetation indices for biomass monitoring in barley. *International Journal of Applied Earth Observation and Geoinformation*, 39, 79-87. <https://doi.org/10.1016/j.jag.2015.02.012>
- Burgess, D. W., Lewis, P., & Muller, J.-P.A.L. (1995). Topographic Effects in AVHRR NDVI Data. *Remote Sensing of Environment*, 54, 223-232. [https://doi.org/10.1016/0034-4257\(95\)00155-7](https://doi.org/10.1016/0034-4257(95)00155-7)
- Huete, A. R. (1988). A soil-adjusted vegetation index (SAVI). *Remote Sensing of Environment*, 25, 295-309. [https://doi.org/10.1016/0034-4257\(88\)90106-X](https://doi.org/10.1016/0034-4257(88)90106-X)
- Myneni, R.B. & Asrar, G. (1994). Atmospheric Effects and Spectral Vegetation Indices. *Remote Sensing of Environment*, 17, 390-402. [https://doi.org/10.1016/0034-4257\(94\)90106-6](https://doi.org/10.1016/0034-4257(94)90106-6)
- Mihaylov, R. (2019). Using drones to track development of maize cultivation. *Farm machinery and Processes Management in sustainable Agriculture, Machinery Equipment, Lublin, Poland 2019*, 43-48. <https://doi.org/10.24326/fmpmsa.2019.1>
- Mihaylov, R., Atanasov, A., Ivanova, A., & Mihaylova, D. (2020). Study of the vegetation of spring crops in the region of South Dobrudzha in 2020. *Annual Journal of Technical University of Varna (AJTUV)*, 4(2),122-129. <https://doi.org/10.29114/ajtuv.vol4.iss2.203>
- Mihajlow, R., & Ivanova, A. (2019). Drone video capture - a new method in precision agriculture. *Annual Journal of Technical University of Varna (AJTUV)*, 3(2) <https://doi.org/10.29114/ajtuv.vol3.iss2.141>
- Rouse, J. W., Haas, R. H., Schell, J. A., Deering, D. W., & Harlan, J. C. (1974). *Monitoring the vernal advancement of retrogradation of natural vegetation*, p. 371. Greenbelt, MD: NASA/GSFC (Type III, Final Report).
- Sankaran, S., Khot, L. R., Espinoza, C. Z., Jarolmasjed, S., Sathuvalli, V. R., Vandemark, G. J., et al. (2015). Low-altitude, high-resolution aerial imaging systems for row and field crop phenotyping: a review. *Eur. J. Agron.*, 70, 112-123. <https://doi.org/10.1016/j.eja.2015.07.004>
- Shi, Y., Thomasson, J. A., Murray, S. C., Pugh, N. A., Rooney, W. L., Shafian, S., et al. (2016). Unmanned aerial vehicles for high-throughput phenotyping and agronomic research. *PLoS One*, 11(7) Article e0159781. <https://doi.org/10.1371/journal.pone.0159781>
- Teillet, P.M., Staenz, K. & Williams, D.J. (1997). Effects of spectral, spatial, and radiometric characteristics on remote sensing vegetation indices of forested regions. *Remote Sensing of Environment*, 61, 139-149. [https://doi.org/10.1016/S0034-4257\(96\)00248-9](https://doi.org/10.1016/S0034-4257(96)00248-9)
- Vincini M., Frazzi, E. & D' Alessio, P. (2008). A broad-band leaf chlorophyll vegetation index at the canopy scale. *Precision Agric*, 9, 303–319. <https://doi.org/10.1007/s11119-008-9075-z>
- Yang, Z., Willis, P. & Mueller, R. (2008). *Impact of band-ratio enhanced AWIFS image to crop classification accuracy*. Pecora 17, 18-20. Department of Health and Ageing. (2012). Aboriginal and Torres Strait Islander health performance framework 2012 report.
- Yang, G., Liu, J., Zhao, C., Li, Z., Huang, Y., Yu, H., et al. (2017). Unmanned aerial vehicle remote sensing for field-based crop phenotyping: current status and Perspectives. *Front. Plant Sci.*, 8, <https://doi.org/10.3389/fpls.2017.01111>

Watson, D.J. (1947). Comparative physiological studies on the growth of field crops: I. Variation in net assimilation rate and leaf area between species and varieties and within and between years. *Annals of Botany.*, 11, 41-76. <https://doi.org/10.1093/oxfordjournals.aob.a083148>

Zhangyan J., Alfredo R.H., Kamel D., & Tomoaki M. (2008). Development of a two-band enhanced vegetation index without a blue band. *Remote Sensing of Environment*, 112 (10), 3833-3845. <https://doi.org/10.1016/j.rse.2008.06.006>

Online sources

Pix4DCapture. (Date of Access 2021), Retrieved from: <https://www.pix4d.com/product/pix4dcapture>

Pix4Dmapper, (Date of Access 2021), Retrieved from: <https://www.pix4d.com/product/pix4dmapper-photogrammetry-software>

Mapir Calibrating Application. (Date of Access 2021), Retrieved from: <https://www.mapir-camera/pages/calibrating-images-in-mapir-camera-control-application>

map.google.com (Date of Access 2021), Retrieved from: <https://www.google.com/maps/@43.548925,27.761216,15z>